

POD Model Order Reduction of electrical networks with semiconductors modeled by the transient Drift–Diffusion equations

Michael Hinze, Martin Kunkel, and Ulrich Matthes

Abstract We consider POD model order reduction (MOR) of integrated circuits with semiconductors modeled by the transient drift-diffusion equations (DDEs). Discretization of the DDEs with mixed finite elements in space yields a high dimensional DAE. We sketch how POD, and POD combined with discrete empirical interpolation (DEIM) can be used to reduce the dimension of the model.

Key words: Model Order Reduction, Reduced Basis Methods, Parametrized Dynamical Systems, Mixed Finite Element Methods, Drift-Diffusion Equations, Integrated Circuits

AMS subject classifications: 93A30, 65B99, 65M60, 65M20

1 Introduction

In this article we investigate a POD-based MOR for semiconductors in electrical networks. In [8] POD-MOR is proposed to obtain a reduced surrogate model conserving as much of the DDEs structure as possible in the reduced order model. This approach in [7] is extended to parametrized electrical networks using the greedy sampling proposed in [10]. Advantage of the POD approach are the higher accuracy

Michael Hinze

Department of Mathematics, University of Hamburg, Bundesstr. 55, 20146 Hamburg, Germany,
e-mail: michael.hinze@uni-hamburg.de

Martin Kunkel

Institute of Mathematics, University of Würzburg, Am Hubland, 97074 Würzburg, Germany,
e-mail: martin.kunkel@mathematik.uni-wuerzburg.de

Ulrich Matthes

Department of Mathematics, University of Hamburg, Bundesstr. 55, 20146 Hamburg, Germany,
e-mail: ulrich.matthes@uni-hamburg.de

of the model and fewer model parameters. On the other hand, numerical simulations are more expensive. For a comprehensive overview of the drift-diffusion equations we refer to [3, 9, 12].

The scaled DDEs are given by

$$\lambda \Delta \psi = n - p - C, \quad (1)$$

$$-\partial_t n + v_n \operatorname{div} J_n = R(n, p), \quad (2)$$

$$\partial_t p + v_p \operatorname{div} J_p = -R(n, p), \quad (3)$$

$$J_n = -\nabla n - n \nabla \psi, \quad (4)$$

$$J_p = -\nabla p - p \nabla \psi, \quad (5)$$

with constants $\lambda := \frac{\varepsilon U_T}{L^2 q \|C\|_\infty}$, $v_n := \frac{U_T \mu_n}{L^2}$ and $v_p := \frac{U_T \mu_p}{L^2}$, where L denotes a specific length of the semiconductor, see e.g. [12]. Semiconductors in electrical networks obtained by a modified nodal analysis are now modeled by the time-discrete version of (1)-(5), which results in a partial DAE of the form

Problem 1 (full model).

$$A_C \frac{d}{dt} q_C (A_C^\top e(t), t) + A_{R_G} (A_R^\top e(t), t) + A_L j_L(t) + A_V j_V(t) + A_S j_S(t) + A_I i_S(t) = 0, \quad (6)$$

$$\frac{d}{dt} \phi_L(j_L(t), t) - A_L^\top e(t) = 0, \quad (7)$$

$$A_V^\top e(t) - v_s(t) = 0, \quad (8)$$

$$j_S(t) - C_1 J_n(t) - C_2 J_p(t) - C_3 \dot{g}_\psi(t) = 0, \quad (9)$$

$$\begin{pmatrix} 0 \\ -M_L \dot{n}(t) \\ M_L \dot{p}(t) \\ 0 \\ 0 \\ 0 \end{pmatrix} + A_{FEM} \begin{pmatrix} \psi(t) \\ n(t) \\ p(t) \\ g_\psi(t) \\ J_n(t) \\ J_p(t) \end{pmatrix} + \mathcal{F}(n^h, p^h, g_\psi^h) - b(e(t)) = 0, \quad (10)$$

where (9) represents the discretized linear coupling condition (11)

$$j_{S,k} = \int_{\Gamma_{O,k}} (J_n + J_p - \varepsilon \partial_t \nabla \psi) \cdot \nu \, d\sigma. \quad (11)$$

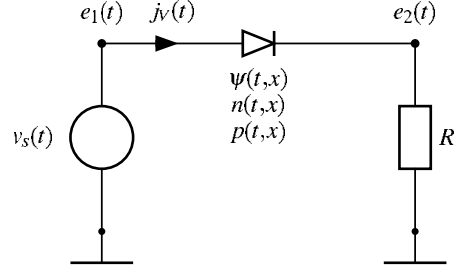
Here, e denotes the node potentials, and j_L and j_V the currents of inductive and voltage source branches, respectively. The electrostatic potential is denoted by $\psi(t, x)$, the electron and hole concentrations by $n(t, x)$ and $p(t, x)$, and the current densities by $J_n(t, x)$ and $J_p(t, x)$. q is the elementary charge, ε the dielectricity, μ_n and μ_p are the mobilities of electrons and holes. The temperature is assumed to be constant which leads to a constant thermal voltage U_T . The function C is the time independent doping profile. We focus on the Shockley-Read-Hall recombination. Furthermore, the incidence matrix $A = [A_R, A_C, A_L, A_V, A_I]$ represents the network topology, e.g. at each non mass node i , $a_{ij} = 1$ if the branch j leaves node i and $a_{ij} = -1$ if the

branch j enters node i and $a_{ij} = 0$ elsewhere. q_C , g and ϕ_L are continuously differentiable functions defining the voltage-current relations of the network components. The continuous functions v_s and i_s are the voltage and current sources. For a basic example consider the network in Fig. 1.

Further details are given in [7]. The analytical and numerical analysis of systems of this form is subject to current research, see [2, 6, 13, 15].

Fig. 1 Basic test circuit with one diode. The network is described by

$$\begin{aligned} A_V &= \begin{pmatrix} 1, & 0 \end{pmatrix}^\top, \\ A_S &= \begin{pmatrix} -1, & 1 \end{pmatrix}^\top, \\ A_R &= \begin{pmatrix} 0, & 1 \end{pmatrix}^\top, \\ g(A_R^\top e, t) &= \frac{1}{R} e_2(t). \end{aligned}$$



2 Model reduction

We use POD-MOR applied to the DD part (10) to construct a dimension-reduced surrogate model for (6)-(10). For this purpose we run a simulation of the unreduced system and collect l snapshots $\psi^h(t_k, \cdot)$, $n^h(t_k, \cdot)$, $p^h(t_k, \cdot)$, $g_\psi^h(t_k, \cdot)$, $J_n^h(t_k, \cdot)$, $J_p^h(t_k, \cdot)$ at time instances $t_k \in \{t_1, \dots, t_l\} \subset [0, T]$. We use the time instances delivered by the DAE integrator. The snapshot variant of POD introduced in [14] finds a best approximation of the space spanned by the snapshots w.r.t. to the considered scalar product. Since every component of the state vector $z := (\psi, n, p, g_\psi, J_n, J_p)$ has its own physical meaning we apply POD MOR to each component separately.

The time-snapshot POD procedure now delivers Galerkin ansatz spaces for ψ , n , p , g_ψ , J_n and J_p and we set $\psi^{POD}(t) := U_\psi \gamma_\psi(t)$, $n^{POD}(t) := U_n \gamma_n(t)$, \dots . The injection matrices $U_\psi \in \mathbb{R}^{N \times s_\psi}$, $U_n \in \mathbb{R}^{N \times s_n}$, \dots , contain the (time independent) POD basis functions, and the vectors $\gamma_{(\cdot)}$ the corresponding time-variant coefficients. The numbers $s_{(\cdot)}$ denote the respective number of POD basis functions included. Assembling the POD system yields a reduced model with similar structure as (6)–(10), see [7] for details. All matrix-matrix multiplications are calculated in an offline-phase. The nonlinear functional \mathcal{F} has to be evaluated online, the arguments have to be interpreted as functions in space. For the reduction of the nonlinearity we use DEIM proposed in [4].

3 Numerical implementation and results

The FEM is implemented in C++ based on the finite element library deal.II [1]. The high dimensional DAE is integrated using the DASPK software package [11].

Fig. 2 Relative error between reduced and unreduced problem at the fixed frequency $5 \cdot 10^9$ [Hz].

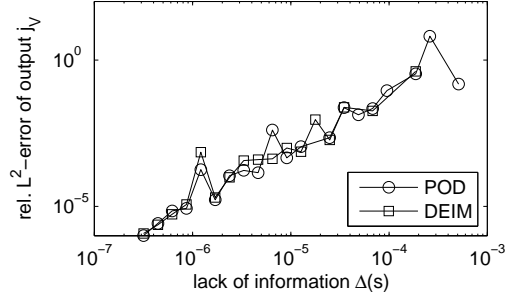
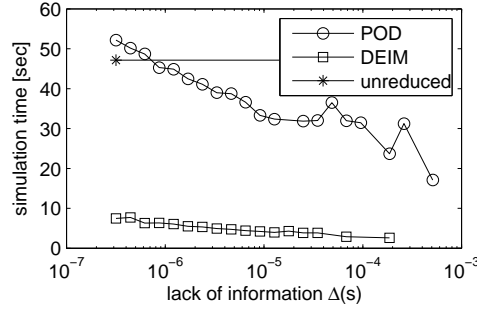


Fig. 3 Time consumption for simulation runs of Fig. 2. The horizontal line indicates the time consumption for the simulation of the original full system.



We assume that the differentiation index of the network is 1. Otherwise one should switch to alternative integrators. The derivative of the nonlinear functional \mathcal{F} with respect to $n_j(t)$, $p_j(t)$, $g_{\psi,j}(t)$ is difficult to compute and thus we calculate the Jacobians by automatic differentiation with the package ADOL-C [16]. We implement the preconditioning subroutine of DASPCK using SuperLU [5].

A basic test circuit with a single 1-dimensional diode is depicted in Fig. 1. The parameters of the diode are summarized in [7]. The input $v_s(t)$ is chosen to be sinusoidal with amplitude 5 [V]. In the sequel the frequency of the voltage source will be considered as a model parameter.

Fig. 2 validates the POD reduced and the POD-DEIM reduced model at the reference frequency of $5 \cdot 10^9$ [Hz] w.r.t. the lack of information Δ . It shows that both reduction techniques perform equally well. The number of POD and DEIM-POD basis functions $s_{(\cdot)}$ for each variable is chosen such that the indicated approximation quality is reached, i.e. $\Delta := \Delta_{\psi} \simeq \Delta_n \simeq \Delta_p \simeq \Delta_{g_{\psi}} \simeq \Delta_{J_n} \simeq \Delta_{J_p}$.

In Fig. 3 the simulation times are plotted versus the lack of information Δ . The POD reduced order model does not reduce the simulation times significantly for the chosen parameters. The reason for this is the dependency on the number of variables of the unreduced system. Here, the unreduced system contains 1000 finite elements which yields 12012 unknowns. The POD-DEIM reduced order model behaves very well and leads to a reduction in simulation time of about 90% without reducing the accuracy of the reduced model. However, we have to report a minor drawback; not all tested reduced models converge for large $\Delta(s) \geq 3 \cdot 10^{-5}$. This is indicated in the figures by missing squares. This effect is even more pronounced for spatially two-dimensional semiconductors.

Fig. 4 The number of required POD basis function and DEIM interpolation indices grows only logarithmically with the requested information content.

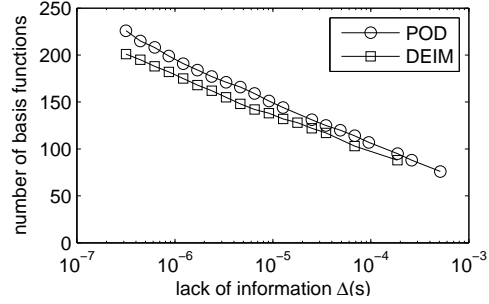
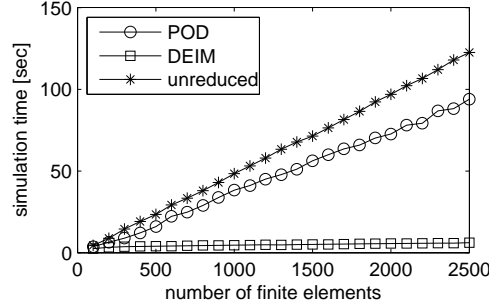


Fig. 5 Computation times of the unreduced and the reduced order models plotted versus the number of finite elements.



In Fig. 4 we plot the corresponding total number of required POD basis functions. It can be seen that with the number of POD basis functions increasing linearly, the lack of information tends to zero exponentially. Furthermore, the number of DEIM interpolation indices behaves in the same way.

In Fig. 5 we investigate the dependence of the reduced models on the number of finite elements N . One sees that the simulation times of the unreduced model depends linearly on N . The POD reduced order model still depends on N linearly with a smaller constant. The dependence on N of our DEIM-POD implementation is negligible.

Finally, we in Fig. 6 analyze the behaviour of the models with respect to parameter changes. We consider the frequency of the sinusoidal input voltage as model parameter. The reduced order models are created based on snapshots gathered in a full simulation at a frequency of $5 \cdot 10^9 [Hz]$. We see that the POD model and the POD-DEIM model behave very similar. The adaptive enlargement of the POD basis using the residual greedy approach of [10] is discussed in [7].

Summarizing all numerical results we conclude that the significantly faster POD-DEIM reduction method yields a reduced order model with the same qualitative behaviour as the reduced model obtained by classical POD-MOR.

Acknowledgements The work reported in this paper was supported by the German Federal Ministry of Education and Research (BMBF), grant no. 03HIPAE5. Responsibility for the contents of this publication rests with the authors.

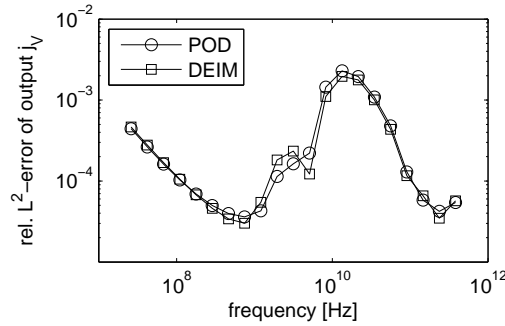


Fig. 6 The reduced models are compared with the unreduced model at various input frequencies.

References

1. Bangerth, W., Hartmann, R., Kanschat, G.: deal.II — a general-purpose object-oriented finite element library. *ACM Trans. Math. Softw.* **33**(4) (2007)
2. Bodestedt, M., Tischendorf, C.: PDAE models of integrated circuits and index analysis. *Math. Comput. Model. Dyn. Syst.* **13**(1), 1–17 (2007)
3. Brezzi, F., Marini, L., Micheletti, S., Pietra, P., Sacco, R., Wang, S.: Discretization of semiconductor device problems. I. Schilders, W. H. A. (ed.) et al., *Handbook of numerical analysis. Vol XIII. Special volume: Numerical methods in electromagnetics*. Amsterdam: Elsevier/North Holland. *Handbook of Numerical Analysis* 13, 317–441 (2005)
4. Charturantabut, S., Sorensen, D.C.: Discrete empirical interpolation for nonlinear model reduction. Tech. Rep. 09-05, Department of Computational and Applied Mathematics, Rice University (2009)
5. Demmel, J.W., Eisenstat, S.C., Gilbert, J.R., Li, X.S., Liu, J.W.H.: A supernodal approach to sparse partial pivoting. *SIAM J. Matrix Analysis and Applications* **20**(3), 720–755 (1999)
6. Günther, M.: Partielle differential-algebraische Systeme in der numerischen Zeitbereichsanalyse elektrischer Schaltungen. *VDI Fortschritts-Berichte, Reihe 20, Rechnerunterstützte Verfahren*, Nr. 343 (2001)
7. Hinze, M., Kunkel, M.: Residual based sampling in pod model order reduction of drift-diffusion equations in parametrized electrical networks. submitted, preprint available at URL <http://arxiv.org/abs/1003.0551> (2010)
8. Hinze, M., Kunkel, M., Vierling, M.: Pod model order reduction of drift-diffusion equations in electrical networks. Accepted for publication in *Lecture Notes in Electrical Engineering*, Vol. 74, Benner, Peter; Hinze, Michael; ter Maten, E. Jan W. (Eds.) (2010)
9. Markowich, P.: *The Stationary Semiconductor Device Equations*. Computational Microelectronics. Springer-Verlag Wien-New York. (1986)
10. Patera, A., Rozza, G.: Reduced basis approximation and a posteriori error estimation for parametrized partial differential equations. version 1.0. Copyright MIT 2006-2007, to appear in (tentative rubric) *MIT Pappalardo Graduate Monographs in Mechanical Engineering* (2007)
11. Petzold, L.R.: A description of DASSL: A differential/algebraic system solver. *IMACS Trans. Scientific Computing* **1**, 65–68 (1993)
12. Selberherr, S.: *Analysis and Simulation of Semiconductor Devices*. Springer-Verlag Wien-New York. (1984)
13. Selva Soto, M., Tischendorf, C.: Numerical analysis of DAEs from coupled circuit and semiconductor simulation. *Appl. Numer. Math.* **53**(2-4), 471–488 (2005)
14. Sirovich, L.: Turbulence and the dynamics of coherent structures I: Coherent structures. II: Symmetries and transformations. III: Dynamics and scaling. *Q. Appl. Math.* **45**, 561–590 (1987)
15. Tischendorf, C.: *Coupled Systems of Differential Algebraic and Partial Differential Equations in Circuit and Device Simulation*. Habilitation thesis, Humboldt-University of Berlin (2003)
16. Walther, A., Griewank, A.: A package for automatic differentiation of algorithms written in c/c++. URL <https://projects.coin-or.org/ADOL-C>